Chapter 4
Carboxysomes and Their Structural Organization in Prokaryotes

Sabine Heinhorst, Gordon C. Cannon and Jessup M. Shively

4.1 Introduction

Following their discovery in the early 1970s, carboxysomes, the CO_2-fixing organelles of many autotrophic bacteria, were largely regarded as oddities, specific to the metabolism of autotrophs and therefore of limited interest to the greater scientific community. After leading an existence in relative obscurity for decades, the genetic potential to form polyhedral protein inclusions related to carboxysomes was discovered throughout the bacterial kingdom. Once the structural similarity of the building blocks from which all of these bacterial microcompartments (BMCs) are constructed was elucidated, the tremendous potential of carboxysomes and related BMCs for synthetic biology and a variety of biotechnological applications was recognized. The ensuing flurry of research activities designed to elucidate and manipulate their structure, function, and biogenesis has led to considerable advances that are documented in several recent reviews (Bobik 2006; Cheng et al. 2008; Yeates et al. 2008; Kerfeld et al. 2010; Yeates et al. 2011; Rae et al. 2013; Yeates et al. 2013). This contribution will concentrate on areas that have not been covered exhaustively, such as insights gained from recent ultrastructural and cell biological approaches, and will focus on structural and functional comparisons between the α-carboxysomes found in many marine cyanobacteria and chemoautotrophs and the β-carboxysomes that occur mainly in freshwater cyanobacteria.

In accordance with the earliest models of carboxysome contribution to autotrophic metabolism, these polyhedral structures constitute a separate compartment within the bacterial cell, in which the important final step of the carbon dioxide-concentrating mechanism (CCM) takes place. The ability to accumulate inorganic

S. Heinhorst (✉) · G. C. Cannon
Department of Chemistry and Biochemistry, The University of Southern Mississippi, 118 College Drive #5043, Hattiesburg, MS 39406-0001, USA
e-mail: Sabine.heinhorst@usm.edu

J. M. Shively
Department of Genetics and Biochemistry, Clemson University, Clemson, SC 29634, USA

L. L. Barton et al. (eds.), *Nanomicrobiology,* DOI 10.1007/978-1-4939-1667-2_4

carbon intracellularly allows autotrophic bacteria to grow efficiently at the low concentrations of available dissolved carbon they encounter in their environment (reviewed in Heinhorst et al. 2006). Carboxysomes, which contain the CO_2-fixing enzyme ribulose 1,5-bisphosphate carboxylase/oxygenase (RubisCO), enhance the catalytic performance of this rather inefficient enzyme by a molecular mechanism that, although not completely understood, relies on contributions of their protein shell and of the carboxysomal carbonic anhydrase to concentrate the RubisCO substrate CO_2 within their interior. Underscoring the importance of carboxysomes for autotrophic metabolism are the numerous mutants that harbor structurally or functionally deficient organelles; the great majority of them have a *h*igh CO_2-*r*equiring or *hcr* phenotype, i.e., they require supplementation with additional CO_2 to achieve growth rates that approach wild-type levels.

4.2 Ultrastructure of Carboxysomes and Their Cellular Associations

The ultrastructure of carboxysomes and their cellular environment have been documented and refined repeatedly since the function of these microcompartments was elucidated in 1973 (Shively et al. 1973a). The early literature is largely based on observations made with thin sections of cells and with isolated carboxysomes that had been fixed and stained in preparation for transmission electron microscopy (TEM). Surprisingly, in spite of the drawbacks and artifacts associated with the harsh treatments to which the specimen were subjected, most of the conclusions reached about shape and diameter of carboxysomes, their number per cell, and the arrangement of RubisCO holoenzymes within the particles have withstood the test of time.

The higher resolution capabilities of modern electron microscopy techniques and instrumentation, combined with milder specimen preparation methods, have since revealed unprecedented ultrastructural details. Of particular importance in this regard has been the ability to obtain three-dimensional images of cellular structures and supramolecular assemblies by cryo-electron tomography (CET). Specimens are frozen rapidly in vitreous ice, a procedure that minimizes damage and preserves molecular structures in a near-in vivo, hydrated state. A series of images, taken at different tilt angles, subsequently forms the basis for the computer-aided reconstruction of biological structures in three dimensions (Tocheva et al. 2010).

In a landmark publication, Nierzwicki-Bauer et al. (1983) reported the three-dimensional ultrastructure of the β-carboxysome-containing unicellular cyanobacterium *Synechococcus* sp. PCC 7002, reconstructed from high-voltage transmission electron micrographs of serial cell sections. Van der Meene et al. (2006) later used a combination of electron microscopy and tomography to establish a three-dimensional model of the β-cyanobacterium *Synechocystis* PCC 6803. Both of these studies, as well as more recent electron tomography work (Ting et al. 2007; Liberton et al. 2011), confirmed the observations that carboxysomes in unicellular cyanobacteria are exclusively located in the central cytoplasm, which is devoid of thylakoid membranes and contains the bacterial DNA and the majority of the ribosomes.

Grouping of carboxysomes was observed in the cyanobacteria *Synechococcus* sp. PCC 7002 (Nierzwicki-Bauer et al. 1983), *Cyanothece* sp. ATCC 51142 (Liberton et al. 2011), *Anabaena* PCC 7119 (Orus et al. 2001), and two *Prochlorococcus* strains (Ting et al. 2007), as well as in the chemoautotrophic sulfur oxidizers *Halothiobacillus neapolitanus,Thiomicrospira crunogena,* and *Thiomonas intermedia* (Iancu et al. 2010). Although the significance of this clustering is not known, Ting et al. (2007) speculated that the close proximity of multiple carboxysomes may allow CO_2 that has diffused out of one carboxysome to be taken up by a neighboring organelle and contribute to efficient CO_2 fixation. Indeed, an increase in nonrandom distribution of carboxysomes was observed in several cyanobacterial species that were placed under carbon limitation conditions (McKay et al. 1993; Orus et al. 2001). Iancu et al. (2010) offered the alternative possibility that carboxysome grouping may reflect a common biogenesis site in the cell or may simply be the consequence of molecular crowding.

Most species have been reported to harbor between 1 and 20 carboxysomes per cell, with average numbers ranging from four to ten (Shively et al. 1973b; Nierzwicki-Bauer et al. 1983; van der Meene et al. 2006; Iancu et al. 2010); in a chemostat culture of the deep sea chemoautotroph *Thiomicrospira crunogena,* more than 80 carboxysomes were observed in some cells (Iancu et al. 2010). Changes in the number of carboxysomes per cell are well documented in the literature for chemo- and photoautotrophic bacteria. In keeping with their role in the CCM, carboxysome numbers increase during carbon limitation and decrease when the bacteria are supplied with elevated levels of CO_2 (Purohit et al. 1976; Beudeker et al. 1980; Pronk et al. 1990; McKay et al. 1993; Orus et al. 2001). For some but not all bacteria, the number of carboxysomes per cell increases significantly during stationary growth phase (Shively et al. 1970; Purohit et al. 1976). Likewise, a correlation of carboxysome numbers with cell size, i.e., the cell division cycle, has been reported (Shively et al. 1973b; Iancu et al. 2010).

4.2.1 Carboxysome Association with Polyphosphate Granules

In transmission electron micrographs of *Synechococcus* sp. PCC 7002 cell thin sections, carboxysomes are seen aligned along the longitudinal cell axis, where they are interspersed and sometimes in direct contact with electron dense, spherical cytoplasmic inclusions (Nierzwicki-Bauer et al. 1983). Elemental analysis by energy dispersive X-ray spectrometry of *Synechococcus leopoliensis* thin sections led to the conclusion that these structures, which are found in many bacteria and some archaea, are polyphosphate (also known as volutin) granules (Tang et al. 1995). Liberton et al. (2011) likewise observed a close association of carboxysomes with polyphosphate bodies in *Cyanothece* sp. ATCC 51142. A recent CET study of three chemoautotrophic sulfur bacteria revealed that their carboxysomes also cluster around cytoplasmic polyphosphate granules (Figure 4.1a), often through direct physical connections that appear to be mediated by unique lattice and string structures emanating from the granules (Iancu et al. 2010). In *H. neapolitanus,* 40 % of

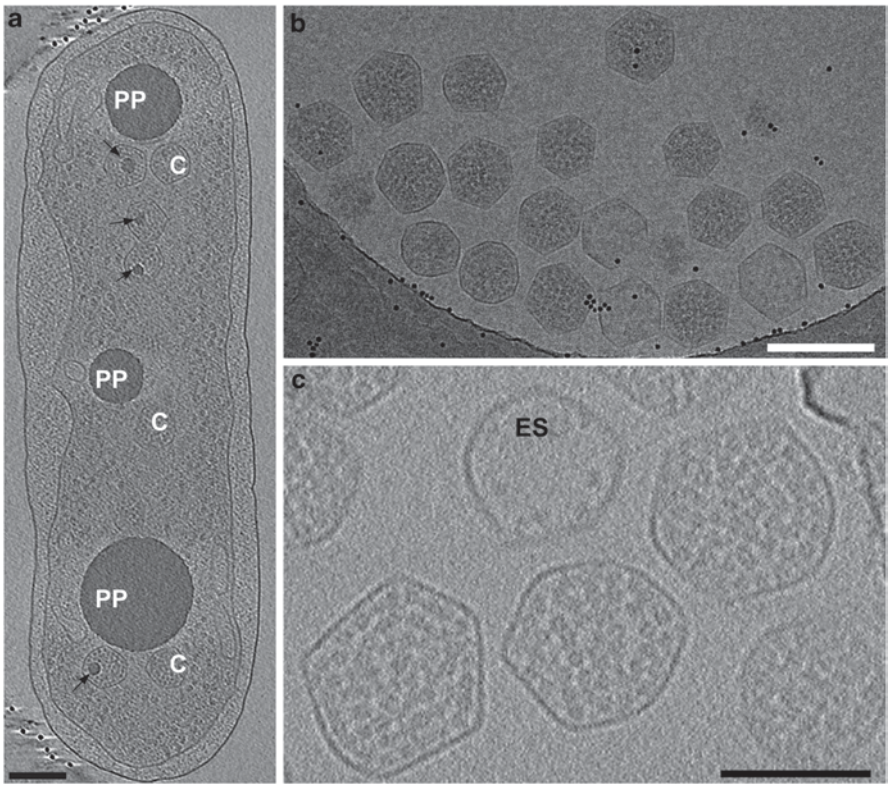

Fig. 4.1 Cryo-electron tomograms. **a** *H. neapolitanus* cell containing several carboxysomes (*C*) and polyphosphate granules (*PP*); some of the carboxysomes have polyphosphate inclusions (*small black arrows*); scale bar = 200 nm. **b** Tomogram of purified *H. neapolitanus* carboxysomes that illustrate the size heterogeneity among individual particles; scale bar = 100 nm. **c** Tomogram of carboxysomes that illustrate the arrangement of individual RubisCO molecules inside; *ES* = empty shell with just a few remaining RubisCO holoenzyme molecules; scale bar = 100 nm. (Images courtesy of Cristina Iancu and Grant J. Jensen)

the cellular carboxysomes were found to be associated with polyphosphate bodies. Interestingly, smaller inclusions of similar densities as the cytoplasmic polyphosphate granules also reside within the carboxysomes of several cyanobacteria (Tang et al. 1995; and references therein) and chemoautotrophs (Figure 4.1a; Iancu et al. 2010). Like their cytoplasmic counterparts, the intra-carboxysomal granules of *Synechococcus leopoliensis* are enriched in phosphorus and contain Ca^{2+}, and probably Mg^{2+} and K^{+} counterions (Tang et al. 1995). To date, a functional relationship between polyphosphate granules and carboxysomes has not been established. Since only a fraction of the carboxysomes within a cell contains polyphosphate inclusions (Tang et al. 1995; Iancu et al. 2010), a direct effect on CO_2 fixation can probably be excluded. Instead, a role as a phosphorus or divalent metal store has

been suggested, particularly in light of the documented decrease in size and abundance of the granules in response to sulfur and phosphate deprivation (Tang et al. 1995; Iancu et al. 2010). *Synechococcus leopoliensis* cells exposed to heavy metals contain an increased number of carboxysomes with polyphosphate granules, which indicates a possible connection to the stress response in this bacterium (Tang et al. 1995). Although not all carboxysomes in a cell harbor polyphosphate granules, considering the importance of phosphorylated intermediates in metabolism, the physiological significance of the observed association of α- as well as β-carboxysomes with polyphosphate bodies begs to be addressed experimentally.

4.2.2 Carboxysome Size Heterogeneity

Compared to the considerable size variations observed among α-carboxysomes in cells of chemoautotrophic bacteria (Figure 4.1a; Iancu et al. 2010), purified particles exhibit only moderate size heterogeneity, with diameters of individual *H. neapolitanus* (Figure 4.1b, c) and *Synechococcus* WH 8102 carboxysomes ranging from less than 100 to more than 160 nm (Schmid et al. 2006; Iancu et al. 2007; Iancu et al. 2010). Using scanning electron microscopy, Schmid et al. (2006) documented mass heterogeneity (100–350 MDa) among purified carboxysomes from *H. neapolitanus*. The extremes of that mass range deviate considerably from the calculated 280 MDa derived from the weight percentages of individual polypeptides in carboxysomes (Cannon and Shively 1983) and from geometric calculations (Shively and English 1991), and are indicative of significant variations in shell composition and/or packaging density of RubisCO between individual particles. Regardless of the observed size and mass heterogeneity, the CET studies (Schmid et al. 2006; Iancu et al. 2007) firmly established an icosahedral geometry for purified α-carboxysomes and resolved the long-standing question regarding their shape (icosahedron vs. pentagonal dodecahedron) that had persisted in the literature for several decades (Peters 1974; Holthuijzen et al. 1986; Shively and English 1991).

The polyhedral shape of carboxysomes led some investigators to suggest early on that they might be related to bacteriophages (Bock et al. 1974; Peters 1974; Westphal and Bock 1974). However, there is no bioinformatic or structural evidence that would indicate a phylogenetic link between carboxysomes and viruses (Kerfeld et al. 2010). Likewise, size and shape heterogeneity of carboxysomes (Figure 4.1; Schmid et al. 2006; Iancu et al. 2007; Iancu et al. 2010) suggests a high degree of compositional flexibility that differs starkly from the monodispersity of virus particles. Careful consideration of shell thickness as a percentage of particle diameter yields a significantly lower number for carboxysomes than for typical viral capsids (Tsai et al. 2007). The thickness of *H. neapolitanus* and *Nitrobacter winogradsky* carboxysome shells is less than 5 % of their particle diameter; by comparison, the corresponding value for cowpea chlorotic mottle virus is approximately 14 % (Shepherd et al. 2006).

4.3 Stability Differences Between Carboxysome Types

While α-carboxysomes can be purified, are stable in vitro, and therefore lend themselves to detailed ultrastructural (Figure 4.1b, c; Schmid et al. 2006; Iancu et al. 2007; Iancu et al. 2010), compositional (Cannon and Shively 1983; Baker et al. 1999, 2000), and functional analysis (Dou et al. 2008; Menon et al. 2008, 2010; Cai et al. 2009; Menon et al. 2010), the same cannot be said for β-carboxysomes. Fractions enriched in β-carboxysomes can be obtained via a Percoll-based coprecipitation method (Price et al. 1992), but the resulting preparations do not appear to be homogeneous and do not lend themselves to exhaustive ultrastructural analysis by electron microscopic methods, such as negative staining TEM or CET, that require large sample numbers to yield meaningful information. In our hands (authors' unpublished observations), electron microscopic analysis of fractions obtained during the purification of carboxysomes from *Thermosynechococcus elongatus* suggests that β-carboxysomes lose their polyhedral structure soon after lysis of the cell. While occasionally an intact β-carboxysome is observed without prior fixation, sample sizes large enough to yield definitive compositional information and draw solid ultrastructural conclusions are not obtained. In contrast, α-carboxysomes appear to be quite robust; sterile samples of *H. neapolitanus* carboxysomes retain their shape and enzymatic activity for at least 5 years when stored at 4 °C. Furthermore, the literature contains numerous examples of electron micrographs in which multiple, apparently homogeneous, intact α-carboxysomes are visible per microscope field. Likewise, 100–200 individual α-carboxysomes were analyzed for CET studies (Figure 4.1b, 4.1c) (Schmid et al. 2006; Iancu et al. 2007; Iancu et al. 2010). To date, comparable studies of intact, purified β-carboxysomes do not exist.

4.4 The Carboxysome Shell

The predominant proteins of the carboxysome shell are small (8–10 kDa) polypeptides that contain a BMC domain (Pfam00936) of approximately 80 amino acids consisting of three α-helices and four β-strands (Kerfeld et al. 2005). The single-BMC-domain proteins, termed CsoS1 in α-carboxysomes and CcmK in β-carboxysomes, self-assemble into hexamers that, in turn, tessellate to form the arrays thought to give rise to the facets of the icosahedral shell (Figure 4.2; (Kerfeld et al. 2005; Tsai et al. 2007; Tsai et al. 2009; Kinney et al. 2011). The tandem-BMC-domain proteins, which are low-abundance shell components, assemble into trimers (pseudohexamers) that are stacked (Figure 4.2; Klein et al. 2009; Kinney et al. 2011; Cai et al. 2013). With the exception of the small marine cyanobacterium *Prochlorococcus marinus* MED4, which is unique in that it utilizes only one single-BMC-domain (CsoS1) and one tandem-BMC-domain (CsoS1D) protein in its carboxysome shell (Figure 4.3; Roberts et al. 2012), the genomes of all other known carboxysome-containing bacteria carry multiple paralogs for single-BMC-domain proteins and at least one gene for a tandem-BMC-domain polypeptide (Figure 4.3)

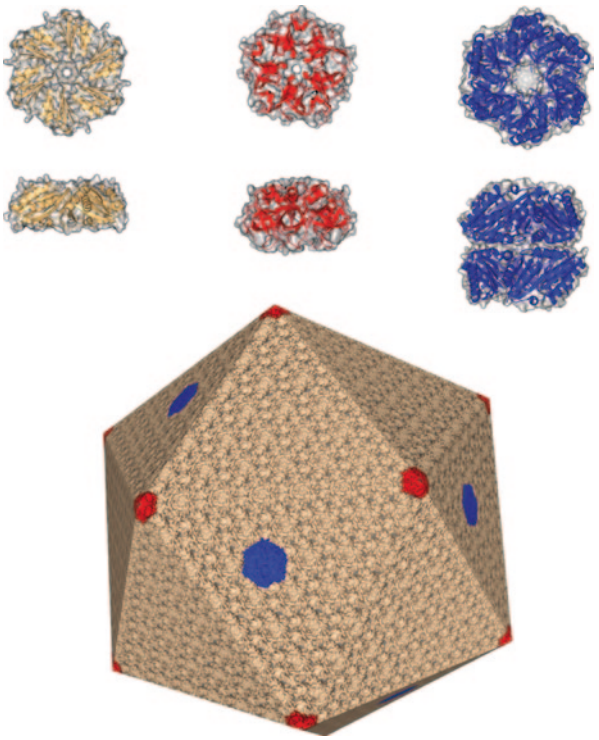

Fig. 4.2 The known building blocks of the carboxysome shell. Hexamers of pfam00936 single-BMC-domain proteins (*wheat*) are the main shell components, thought to form the facets of the icosahedral particles. Pentamers of pfam03319 proteins (*red*) are believed to occupy the vertices. Pseudohexamers of pfam00936 tandem-BMC-domain proteins (*blue*), some of which assemble into stacked dimers of trimers, are low-abundance shell constituents. Shown are models based on α-carboxysome shell components (from left to right 2G13, 2RCF, and 3F56). (Image courtesy of Fei Cai and Cheryl Kerfeld)

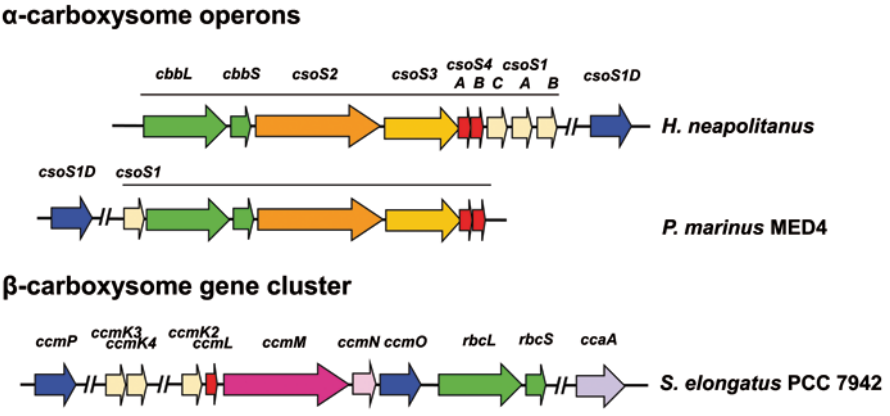

Fig. 4.3 Gene clusters encoding proteins of α- and β-carboxysomes. Shown are the *cso* operons of *Prochlorococcus marinus* MED 4 and *Halothiobacillus neapolitanus* including the *csoS1D* genes that are not part of the operons, and the carboxysome gene clusters of *Synechococcus elongatus* PCC 7942. The colors of the genes encoding the major shell components are the same as those in Figure 4.2 (*wheat, red,* and *blue*). The genes for the large and small subunits of Form I RubisCO are *green*

(Kinney et al. 2011). Members of an additional shell protein family (Pfam03319) are the constituents of the pentamers thought to occupy the vertices of the polyhedral carboxysomes (Figures 4.2 and 4.3; Tanaka et al. 2008; Kinney et al. 2011). Orthologous genes encoding these two protein families are found throughout many bacterial lineages in approximately one fifth of all sequenced bacterial genomes. Some of these bacteria have been shown to form BMCs of similar structure, but unrelated function, that encapsulate enzymes necessary for the catabolism of certain carbon sources (reviewed in Kerfeld et al. 2010). Clearly, protein shell-based compartmentalization of the enzymes that catalyze selected biochemical reactions appears to be a widespread metabolic strategy among the bacteria.

4.4.1 Single Pfam00936 Shell Proteins

The *cso* operons of *H. neapolitanus,Thiomonas intermedia,* and *Thiomicrospira crunogena* each encode three single-BMC-domain proteins (CsoS1) that share a high degree of sequence similarity and differ in only a few residues throughout the length of their common regions (Figure 4.3). The CsoS1B protein of *H. neapolitanus* features a C-terminal extension of 12 amino acids that is not present in its CsoS1A and CsoS1C paralogs (Cannon et al. 2003) and may be important for carboxysome assembly and/or interaction with proteins located on the interior face of the shell (see below).

The genomes of the model β-cyanobacteria *Synechocystis* sp. PCC6803 and *Synechococcus elongatus* PCC7942 (Figure 4.3) harbor genes for four and three single-BMC-domain paralogs, respectively. Individual CcmK paralogs, like their α-carboxysomal orthologs, have very similar core sequences but differ in their C-termini (Tanaka et al. 2009). Although the protein complement of β-carboxysomes has not been unequivocally determined, proteomic analysis of fractions highly enriched in β-carboxysome proteins (Long et al. 2005, Long et al. 2007, Long et al. 2010) and the phenotypes of various mutants (Savage et al. 2010; Rae et al. 2012 and references therein) have permitted an assessment of the likely shell constituents. In *Synechococcus elongatus* PCC 7942, CcmK2 appears to be the most abundant single-BMC-domain protein that is consistently identified in enriched fractions (Long et al. 2005, Long et al. 2007; Long et al. 2010). Furthermore, *ΔccmK2* mutants are devoid of carboxysomes, a phenotype that establishes this protein as an essential constituent of the β-carboxysome shell (Rae et al. 2012; Cameron et al. 2013). Fluorescently tagged CcmK4 protein of *Synechococcus elongatus* PCC7942 localizes to the punctate structures thought to represent individual carboxysomes (Savage et al. 2010). This protein and its paralog CcmK3 do not seem to be structurally important components of the β-carboxysome shell but rather contribute to organelle function (Zhang et al. 2004; Rae et al. 2012).

Whether the carboxysome shell in those bacteria that express multiple single-BMC-domain proteins contains homo-hexamers consisting of only one type of monomer or is comprised of hexamers that feature combinations of different

paralogs is not known. Hexamers formed by individual β-carboxysomal CcmK paralogs are nearly identical in shape and are easily superimposable, with the exception of the C-terminal extensions found in some paralogs (Tanaka et al. 2009). Although they do not address the homo-versus hetero-hexamer question, the fluorescence resonance energy transfer (FRET) approaches employed by Samborska and Kimber (Samborska and Kimber 2012) are the first to directly probe interactions between pairs of BMC-domain protein paralogs. The authors showed that *Thermosynechococcus elongatus* CcmK2 preferentially interacts with itself. The CcmK1 and CcmK4a proteins, however, have higher affinity for specific paralogs than for themselves. Whether this result is indicative of interactions within hetero-hexamers or between homohexamers of different paralogs is not clear. One can speculate that hetero-hexamers would expand the repertoire of potential contacts and attachment points for cargo proteins within the carboxysome, and/or with extra-organellar structures on the cytosolic side that might be relevant for carboxysome function and/or intracellular distribution.

Based on molecular models derived from crystallographic data, each hexamer possesses a convex and a concave side of different surface charge (reviewed in Kinney et al. 2011). All hexamers are predicted to be oriented in the same manner in the shell (Tanaka et al. 2008), but the sidedness of the arrays is an as-yet unresolved question. The surface that presents itself to the cytosolic side is likely important for the recruitment of metabolites to the carboxysome, their transfer across the shell, and interactions with other cellular structures, while the inward-facing surface engages in contact with the encapsulated proteins. Direct experimental evidence is needed to determine which side of the BMC-domain protein assemblies faces the inside and the outside of the carboxysome to advance our understanding of the way in which shell structure and architecture are related to function.

Each shell protein hexamer contains a central pore of a diameter that varies from 4 to 7 Å, depending on the monomer constituent (Figure 4.2; reviewed in Kinney et al. 2011). Given the tight interactions between individual subunits within a hexamer and between neighboring hexamers and the invariably positive surface charge of the openings, the pores have been proposed to represent the main route for the flux of the negatively charged RubisCO substrates and products into and out of the carboxysome (Kerfeld et al. 2005; Tsai et al. 2007; Tanaka et al. 2008). If this assumption is proven to be correct, the pore structure/function relationship forms the basis for the selective shell permeability that appears to be a crucial determinant of carboxysome function in the bacterial CCM (Reinhold et al. 1989; Kaplan and Reinhold 1999; Dou et al. 2008). Although sulfate (Kerfeld et al. 2005; Tsai et al. 2007; Samborska and Kimber 2012) and glycerol (Samborska and Kimber 2012) can be trapped in crystals of single-BMC-domain protein crystals, the molecular mechanism by which the pores might provide the requisite selective permeability and impede the diffusion of CO_2 is not obvious. It is tempting to suggest that metabolite transfer might operate through a protein channel-like mechanism reminiscent of that found in aquaporins (de Groot and Grubmuller 2005). One may also speculate that the monomer composition of individual hexamers could exert an effect on the characteristics of the pore. Although the residues that line the pores are

highly conserved among paralogs, the presence of different paralogs in a hexamer may lead to subtle yet significant variations in pore structure; these could broaden the range of small molecules able to cross the carboxysome shell or, alternatively, restrict access of certain metabolites to the carboxysome interior. A complicating factor in proposing a convincing mechanism for metabolite transfer across the carboxysome shell is the small size of the hexamer pores. Although wide enough for the passage of bicarbonate and Mg^{2+}, it is difficult to envision how the considerably larger RubP and 3-phosphoglyceric acid (3-PGA) molecules could effectively traverse the shell through such narrow passages, despite some apparent structural flexibility of the pore (Samborska and Kimber 2012).

4.4.2 Tandem Pfam00936 Shell Proteins

Recently, the tandem-BMC-domain proteins have emerged as possible candidates that might mediate passage of larger metabolites across the carboxysome shell. Discovered originally in the genome of *P. marinus* MED4, the gene encoding such a protein was termed *csoS1D* to indicate the structural relationship of its product to the single-BMC-domain proteins (Figure 4.3). Orthologs exist in all cyanobacteria (Klein et al. 2009; Cai et al. 2013) and in carboxysome-forming chemoautotrophs (Roberts et al. 2012; Figure 4.3). Interestingly, the *csoS1D* genes of α-carboxysome-forming bacteria are not part of their *cso* operons (Figure 4.3); however, expression of *csoS1D* appears to respond to carbon availability in the same manner as the canonical carboxysome genes in *P. marinus* MED4 (Klein et al. 2009).

The two BMC domains of CsoS1D and its orthologs, although bearing little amino acid sequence similarity, are structurally almost identical and assemble into stacked dimers of pseudohexameric trimers (Figure 4.2; Klein et al. 2009; Cai et al. 2013). The pores of the trimers are considerably larger (14–15 Å diameter) than those of the hexamers formed by single-BMC-domain proteins and could easily accommodate the larger RubisCO substrate and product molecules (Klein et al. 2009; Cai et al. 2013). Furthermore, the CcmP protein was recently shown to have some affinity for 3-PGA (Cai et al. 2013), a finding that supports a role for tandem-BMC-domain proteins as conduits for the transfer of larger metabolites across the shell. Roberts et al. (2012) identified the CsoS1D protein in purified *P. marinus* MED4 α-carboxysomes and showed that it is tightly associated with the shell, as had been predicted based on models that revealed a tight fit of CsoS1D trimers within CsoS1 hexamer arrays (Figure 4.2; Klein et al. 2009). Cai and coworkers (Cai et al. 2013) solved the structure of the CcmP protein and, using fluorescently tagged protein, showed that CcmP colocalizes with RubisCO to the β-carboxysomes of *Synechococcus elongatus* PCC7942 (Figure 4.4).

Carboxysome tandem-BMC domain protein assemblies have two intriguing structural features with potentially important implications for the mechanism by which carboxysomes communicate and exchange small molecules with their

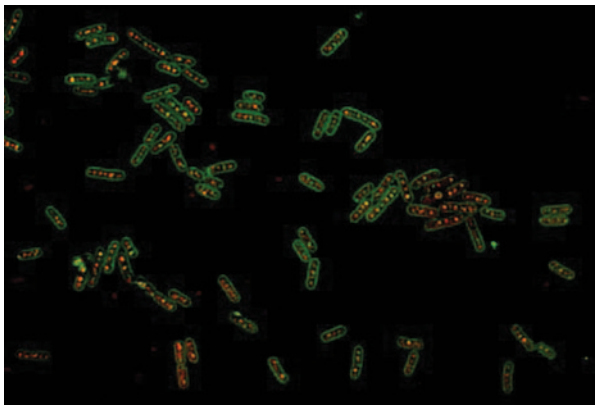

Fig. 4.4 Fluorescently labeled β-carboxysomes in *Synechococcus elongatus* PCC 7942. The cells express fusions of the large subunit of RubisCO with cyan fluorescent protein (*CFP*; *pseudo-color red*) and of shell protein CcmP with yellow fluorescent protein (*YFP*; *pseudo-color green*). Both fluorescent fusion proteins colocalize to bright punctae that are spaced evenly along the long axes of the cells and believed to represent individual carboxysomes. (Image courtesy of Fei Cai and Cheryl Kerfeld)

exterior. The first is an interior channel of predominantly positive surface potential that was first observed in the stacked dimers of *P. marinus* MED4 CsoS1D trimers (Figure 4.3; Klein et al. 2009). Structural analysis of CcmP revealed the existence of a similar nanocompartment within the assembly of this protein; its cavity was also shown to display weak affinity for the product of the RubisCO reaction, 3-PGA (Cai et al. 2013). Secondly, the large trimer pores of tandem BMC-domain proteins can exist in two different states through alternative side-chain conformations of two absolutely conserved residues (Glu and Arg) that that are found in all tandem-BMC proteins identified bioinformatically (Figure 4.3; Klein et al. 2009; Cai et al. 2013). These two amino acids are responsible for gating the two pores of the stacked trimers, one of which tends to be closed while the other one is in the open state in CsoS1D and CcmP crystals (Klein et al. 2009; Cai et al. 2013). Considering the metabolic steps downstream from the carboxylation reaction catalyzed by RubisCO, these nanocompartments within the carboxysome shell could act as temporary reservoirs for RubP and/or 3-PGA. Import into and/or release from the carboxysome of these metabolites could be regulated through gating of the pores in response to the metabolic state (e.g., energy charge, redox poise) of the cell. The one important caveat to this elegant model is the very low abundance of the CsoS1D protein in the *P. marinus* MED4 carboxysome, which is estimated to contain 12 trimers or 6 dimers of stacked trimers that correspond to only 6 nanocompartments with 12 gated pores per particle (Roberts et al. 2012). Each carboxysome has an estimated 740 to more than 1000 pores for bicarbonate (Iancu et al. 2007; Tanaka et al. 2008) provided by the single-BMC domain hexamers. Whether a sufficiently high flux of RubP and/or 3-PGA through the predicted tandem-BMC domain "transporters" can be achieved to support the enzymatic activity of the ~270 fully activated RubisCO holoenzyme molecules in the interior awaits experimental evidence.

4.4.3 *Pfam03319 Shell Proteins*

The geometric requirement for 12 pentamers to close the 20 facets of an icosahedron is believed to be satisfied in both α- and β-carboxysomes by proteins belonging to Pfam03319. The CsoS4 paralogs in α-carboxysomes and CcmL in β-carboxysomes are low-abundance components of the shell that self-associate into pentamers (Figure 4.2). In models of the icosahedral carboxysome shell, the molecular dimensions of the pentamers, calculated from crystallographic data, fit precisely into the proposed vertices (Tanaka et al. 2008). Mutants that do not express vertex proteins have the *hcr* phenotype and produce an increased number of elongated carboxysomes in addition to many particles of apparently normal icosahedral shape (Price et al. 1993; Cai et al. 2009; Rae et al. 2012; Cameron et al. 2013). Since most of the carboxysomes purified from a *H. neapolitanus csoS4A/csoS4B* null mutant appear morphologically similar to wild-type particles, the remaining (Pfam00936) shell proteins appear to be able to close the hexamer arrays of the facets into a three-dimensional icosahedron (Cai et al. 2009).

4.4.4 *Is the Shell Single- or Double-Layered?*

Most ultrastructural studies of carboxysomes have concluded that the bounding shell is a 3–4-nm-thick protein monolayer (Shively et al. 1973; Peters 1974; Holthuijzen et al. 1986; Schmid et al. 2006). However, recent structural analysis of *Thermosynechococcus elongatus* CcmK2 assemblies, combined with elegant FRET analyses, revealed that the concave faces of two of its hexamers associate to form a double-layered dodecamer in vitro (Samborska and Kimber 2012). Since CcmK2 is the only paralog present in all β-carboxysome-forming cyanobacteria, the BMC domain protein that is consistently recovered in β-carboxysome-enriched fractions and an essential carboxysome component (Rae et al. 2012; Cameron et al. 2013), models of the β-carboxysome shell that take into account these hexamer interactions suggest that its facets might consist of a double layer formed by CcmK2 dodecamers (Samborska and Kimber 2012). However, consideration of the fit of the CcmP trimer in the hexamer arrays of CcmK2, on the other hand, favors a single-layered β-carboxysome shell (Cai et al. 2013). Whether the CcmK2 dodecamers observed in vitro reflect the organization of this protein in the carboxysome shell in vivo or possibly represent an early assembly intermediate, as was offered as an alternative suggestion (Samborska and Kimber 2012), awaits further experimental evidence.

4.5 Shell-Associated Proteins

4.5.1 *Shell-Associated Proteins of α-Carboxysomes*

When purified α-carboxysomes are subjected to mild denaturants or mechanical shear, a fraction of the shells breaks and releases the carboxysomal RubisCO into

the surrounding buffer. Although no longer intact, the broken shells tend to retain their shape and can be separated from unbroken carboxysomes and free RubisCO by density gradient centrifugation. This fraction consistently contains the stoichiometric amounts of CsoS1 and CsoS4 paralogs expected from the polypeptide pattern of purified carboxysomes (reviewed in Heinhorst et al. 2006), as well as the CsoS2A and CsoS2B polypeptides and the carbonic anhydrase CsoSCA. In addition, approximately 20 % of the total carboxysomal RubisCO protein complement usually remains with the broken shell fraction and is not released by additional washes (Heinhorst et al. 2006; Schmid et al. 2006; Iancu et al. 2010), suggesting that the outermost RubisCO layer engages in strong interactions with the shell.

The *csoS3* gene of the *cso* operon encodes the CsoSCA protein, the apparently sole CA of α-carboxysomes (reviewed in Cannon et al. 2010). The protein is a unique β-class enzyme whose identity had long remained obscure because of an almost complete lack of primary structure homology to other CAs (Sawaya et al. 2006; Cannon et al. 2010; Kerfeld et al. 2010). Of the three distinct domains revealed in its crystal structure, the middle and C-terminal domains appear to have arisen by an ancient gene duplication event but have since diverged considerably. Only the C-terminal domain carries a binding site for the obligatory zinc ion found in β-CAs and has catalytic activity (Sawaya et al. 2006). The likely in vivo form of CsoSCA is a dimer, which is present in the carboxysome in an estimated 40 copies (Heinhorst et al. 2006). The CsoSCA protein is tightly associated with the shell (Baker et al. 2000; So et al. 2004; Heinhorst et al. 2006; Dou et al. 2008) and, to be stripped from isolated shells, requires increasingly harsh denaturing conditions that release enzymatically inactive CsoSCA protein only as the entire shell dissolves (Heinhorst et al. 2006).

The structural basis for the strong association of CsoSCA with other shell components and the identity of its interaction partners are unknown. There is no obvious fit of the CsoSCA dimers within the tight CsoS1 hexamer arrays or at the vertices of the carboxysome. Since recombinant CsoSCA supplied externally to purified *H. neapolitanus ΔcsoS3* carboxysomes does not rescue the compromised CO_2 fixation ability of the mutant organelles, the enzyme likely faces inward (Dou et al. 2008), as predicted also for the β-carboxysomal CAs CcaA and CcmM (see below; Long et al. 2007; Cot et al. 2008). Although CsoSCA clearly is an important functional component of the α-carboxysome, a significant role of this protein in carboxysome biogenesis and shell structure can be excluded because the carboxysomes of a *H. neapolitanus ΔcsoS3* mutant are indistinguishable from wild-type particles in morphology and protein content, other than lacking the CsoSCA protein (Dou et al. 2008).

Like CsoSCA, the CsoS2 protein of α-carboxysomes does not have an ortholog in β-carboxysomes (Cannon et al. 2002). The largest known constituent of α-carboxysomes remains associated with the shell upon carboxysome disruption and is released only under conditions that lead to disintegration of the entire shell structure (Baker et al. 1999; Heinhorst et al. 2006). The CsoS2 protein has several unique properties. In some bacteria, including *H. neapolitanus,* the protein exists in two forms that share the same N-terminus but may be differentially glycosylated (Baker et al. 1999). The primary structure of the protein features multiple repeat

motifs consisting of three and seven or eight amino acids, as well as a series of conserved Cys residues (Cannon et al. 2003). Since expression of soluble recombinant CsoS2 protein has proven difficult (authors' unpublished observations), no crystal structure is available to date. Its high pI (>9) distinguishes CsoS2 from the remaining known α-carboxysome proteins and suggests that the protein might participate in the transfer of the negatively charged substrate and/or products across the carboxysome shell. However, to date, there is no experimental evidence for a role of CsoS2 in metabolite flux. Given the size of the protein and its unusually high pI, it is tempting to speculate that CsoS2 might be arranged inside the shell, where it could act as molecular "glue" that reinforces the thin layer of BMC-domain protein hexamers. In addition or alternatively, CsoS2 may connect the proximal layer of RubisCO, which remains attached to broken shells (Heinhorst et al. 2006; Iancu et al. 2010) to the inside of the single-BMC domain protein hexamer arrays.

4.5.2 Shell-Associated Proteins of β-Carboxysomes

Contrary to α-carboxysomes, β-carboxysomes are yet to be purified to homogeneity. Since their composition and the stoichiometric ratios of their protein components are not known, their internal organization has been inferred from a combination of genetic, biochemical, and proteomic approaches. The protein encoded by the *ccmM* gene, which does not have a homolog in α-carboxysome forming bacteria, is a crucial component of β-carboxysomes. Gene knockouts yield Δ*ccmM* mutants that do not form carboxysomes and have an absolute requirement for elevated CO_2 (*hcr* phenotype; Ludwig et al. 2000; Berry et al. 2005; Long et al. 2011). The gene encodes at least two protein products in vivo (Price et al. 1998; Long et al. 2005): The full-length polypeptide consists of an N-terminal domain with homology to the γ-carbonic anhydrase Cam from *Methanosarcina thermophila* (Alber and Ferry 1994) and of a C-terminal region featuring multiple repeats with similarity to the small subunit of RubisCO (RbcS; Price et al. 1993; Ludwig et al. 2000). A second, shorter protein product consisting of only the C-terminal RbcS-like repeats is translated from an internal start codon (Long et al. 2007; Long et al. 2011), is present in higher copy number than the full-length version in carboxysome protein-enriched cellular fractions (Long et al. 2011), and is also needed for the assembly of functional carboxysomes in *Synechococcus elongatus* PCC 7942 (Long et al. 2010). Yeast two-hybrid analysis with recombinant proteins that are predicted to be components of the *Synechocystis* sp. PCC 6803 carboxysome revealed interactions between the N-terminal domain of CcmM, the CcmN protein, and CcaA (Cot et al. 2008) and led the authors to propose the existence of a bicarbonate dehydration complex in β-carboxysomes. An assembly consisting of CcmM trimers, CcaA dimers, and CcmN is thought to interact with the outermost RubisCO layer via the C-terminal RbcS-like repeats of CcmM and to rapidly equilibrate entering bicarbonate with CO_2. This model was confirmed by additional protein interaction studies and was subsequently expanded to include a role of the shorter form of CcmM as an organizer of RubisCO in the carboxysome interior (Long et al. 2007, 2010, 2011; Cot

et al. 2008; Peña et al. 2010). Kinney et al. (2012), however, did not find evidence for the presence of CcaA in complexes of CcmM, RubisCO, and the carboxysome protein CcmN the authors isolated using similar immunoprecipitation experiments.

The *ccaA* (*icfA*) gene, which is found in many, but not all, β-carboxysome-containing cyanobacteria, encodes a β-CA that co-purifies with other β-carboxysome proteins during enrichment procedures (So and Espie 1998; So et al. 2002; Cot et al. 2008). Like its α-carboxysomal counterpart CsoSCA, the CcaA protein does not seem to be an important structural component of β-carboxysomes; however, its enzymatic activity is essential for organelle function. Although its carboxysomes are indistinguishable from wild-type organelles in transmission electron micrographs of cell thin sections, *ccaA* null mutants exhibit an *hcr* phenotype (So et al. 2002). The N-terminal portion of CcaA harbors its catalytic domain, which requires dimerization via the C-terminal domain for enzymatic activity and for interaction of CcaA with CcmM (So et al. 2002; Cot et al. 2008).

The absence of a *ccaA* gene from the genomes of several β-carboxysome forming cyanobacteria begged the question whether another carbonic anhydrase exists that is present in all β-carboxysomes. Catalytic activity of the obvious candidate, CcmM, had eluded detection in assays of purified recombinant protein and of *Escherichia coli* extracts expressing CcmM from several cyanobacteria (Cot et al. 2008). Peña et al. (2010) solved the structure of a CcmM fragment from *Thermosynechococcus elongatus* BP-1 that consists of the first 209 amino acids. The authors showed that the CA activity of the protein depends on the oxidized state of a crucial disulfide bond in the catalytic domain. A reducing environment like the cytosol disrupts the structure of the trimeric enzyme and prompts the suggestion that the carboxysome interior is able to maintain an oxidizing milieu in which CcmM is active. A recent study of β-carboxysome biogenesis lends support to this hypothesis by providing evidence for the oxidation of the carboxysome interior as the organelle ages (Chen et al. 2013). Although the CcmM protein appears to be a universal organizing component of all β-carboxysomes, its CA activity seems to have been replaced by that of CcaA in those cyanobacteria that also carry a *ccaA* gene (Peña et al. 2010).

Another gene unique to β-cyanobacteria, *ccmN,* is part of the cluster that includes *ccmM,ccmL,ccmO,ccmK2,* and the RubisCO genes in *Synechococcus elongatus* PCC 7942 (Figure 4.3). Like the *Δ*ccmM mutant, the *ccmN* knockout does not grow at ambient CO_2 concentration (*hcr* phenotype) and, instead of carboxysomes, contains a large polar body that is thought to consist of aggregated protein (Kinney et al. 2012). Fluorescently tagged CcmN protein colocalizes with RubisCO to the distinct punctate structures in the cell thought to represent individual carboxysomes (Kinney et al. 2012). A bioinformatic analysis of CcmN orthologs revealed that the protein contains two conserved regions. The N-terminal portion, which consists of six bacterial hexapeptide repeats (Pfam00132), is predicted to be structurally similar to the CcmM N-terminal region (Peña et al. 2010; Kinney et al. 2012) and was shown to interact with CcmM in pulldown assays that feature CcmN as bait. A conserved C-terminal peptide of 18 amino acids, which is connected to the N-terminal region of CcmN through a variable Pro- and Ser-rich linker, interacts with the shell protein CcmK2. A mutant of *Synechococcus elongatus* PCC 7942 producing CcmN

that is devoid of these 18 amino acids has a similar phenotype as the *ccmN* null mutant, emphasizing the importance of this portion of the protein for carboxysome formation (Kinney et al. 2012). Interestingly, a search for bacterial genomes that carry orthologs of the common BMC shell genes (Pfam00936 and Pfam03319) identified peptides similar to the C-terminal peptide of CcmN in many proteins thought to be targeted to the interior of BMCs. This finding raises the interesting possibility that BMC proteins carrying such a peptide may recruit other proteins to the nascent organelle or contribute to the assembly of the BMC shell itself through interactions with conserved structural elements of shell components (Kinney et al. 2012).

4.6 Shell Permeability

Throughout the evolution of a working model for carboxysome function, various permeability properties have been attributed to the protein shell that could support the proposed role of the carboxysome in the CCM (reviewed in Heinhorst et al. 2006). Clearly, the enzymatic action of the carboxysomal carbonic anhydrase plays a pivotal role in providing the encapsulated RubisCO with a sufficiently high concentration of its substrate CO_2 to ensure efficient CO_2 fixation. Carbon dioxide fixation assays performed with purified *ΔcsoS3* mutant carboxysomes of *H. neapolitanus* revealed a requirement of the encapsulated RubisCO for elevated inorganic carbon levels that was not observed in assays performed with broken mutant organelles. These kinetic measurements provided direct experimental evidence that the shell impedes diffusion of CO_2 (Dou et al. 2008), as had been predicted in the original CCM model (Reinhold et al. 1989). Likewise, carbonic anhydrase activity assays performed with intact purified carboxysomes devoid of the vertex proteins CsoS4A and CsoS4B established that their shells, although of apparently normal polyhedral appearance, are much more permeable to CO_2 than those of wild-type carboxysomes, a functional deficiency that explains the requirement of the mutant for elevated CO_2 levels and lends further support to the proposed role of the shell as a CO_2 diffusion barrier (Cai et al. 2009).

In an attempt to reconcile the common building principles of all BMC shells with a universal function of these bacterial organelles, Penrod and Roth proposed that the interior of all BMCs might provide an environment with a lower pH than that of the cytosol (Penrod and Roth 2006). In the carboxysome interior, a lower pH would benefit CO_2 fixation by shifting the equilibrium between bicarbonate and CO_2 in favor of the RubisCO substrate, and could explain at least in part the advantage RubisCO derives from compartmentalization. However, experiments employing a fusion protein that consists of a pH-sensitive GFP variant and the small subunit of RubisCO did not reveal a pH differential between the inside of the organelle and the cytosol. Unlike the lipid bilayer-based borders that separate eukaryotic cell compartments, the protein shell of the carboxysome is freely permeable to protons (Menon et al. 2010).

4.7 The Arrangement of RubisCO Within the Carboxysome

Transmission electron micrographs presented in the earliest reports of carboxysomes (Gantt and Conti 1969; Shively et al. 1973b) suggested that some particles contain a core of highly ordered RubisCO that is arranged in what was termed a paracrystalline array. However, perusal of a large number of TEM images, each containing many negatively stained, purified α-carboxysomes per field, suggests that paracrystalline structures are rather rare (authors' unpublished observations). Likewise, exhaustive CET analysis of α-carboxysomes, both purified and within intact cells, does not support the paracrystalline model as the most prevalent and biologically significant packing of RubisCO in the icosahedral particles (Figure 4.1; Schmid et al. 2006; Iancu et al. 2007, 2010). Instead, most of the RubisCO holoenzyme molecules were found to be arranged in a layer abutting the inside of the shell. The remaining enzyme molecules occupy two or three additional concentric layers, with RubisCO packing becoming less tight and ordered towards the center of the carboxysome (Figure 4.2). A preferential orientation of individual RubisCO molecules, as one would expect to see in a paracrystalline array, was not discernible. The basis for the rare occurrence of regular RubisCO arrays in α-carboxysome preparations is a mystery that might, however, be related to the tendency of carboxysomal RubisCO molecules to orient themselves on electron microscope grids in highly concentrated preparations (Shively et al. 1973b); Orus et al. 1995; and authors' unpublished observations). Since carboxysomes that are filled to varying degrees with RubisCO are well documented (Schmid et al. 2006; Iancu et al. 2007, 2010), maybe the regular array of RubisCO seen in the occasional carboxysome reflects a particle with particularly densely packed contents.

The arrangement of RubisCO in the interior of β-carboxysomes may be different. Gantt and Conti (Gantt and Conti 1969) reported that some polyhedral bodies observed in negatively stained, cell-free preparations of *Synechococcus elongatus* (formerly *Anacystis nidulans*) appeared as crystalline bodies. More recently, Kaneko et al. (2006) employed Hilbert differential contrast electron microscopy to examine rapidly frozen cells of *Synechococcus elongatus* PCC 7942 and stated about the resulting micrographs: "Occasionally the paracrystalline arrangement of particles could be recognized." It is difficult to assess the proportion of the cellular carboxysomes that contain regularly packed RubisCO and the extent to which the paracrystalline RubisCO arrangement represents the carboxysome interior. Perhaps the highly ordered structures seen in the Hilbert images represent only the outermost layer of RubisCO that is attached to the inside of the shell. Unfortunately, current CET methods do not allow high-resolution studies of intact bacterial cells as large as most cyanobacteria that contain β-carboxysomes; elucidation of RubisCO packaging in these carboxysomes awaits the development of a purification method.

4.8 Carboxysome Assembly

In contrast to the moderate size and mass heterogeneity exhibited by populations of purified α-carboxysomes, CET revealed a considerably greater variation in size and shape among particles within intact cells of the chemoautotrophs *H. neapolitanus,Thiomonas intermedia,* and *Thiomicrospira crunogena* (Iancu et al. 2010) that are suggestive of a considerable structural flexibility of the shell. Occasionally, moderately to greatly elongated carboxysomes, as well as irregularly shaped microcompartments can be seen in cells next to normal icosahedral particles (Gantt and Conti 1969; Shively et al. 1970, 1973b; Iancu et al. 2010). It is not yet known how these aberrantly shaped carboxysomes come to be or, for that matter, how the regular icosahedral shape of carboxysomes arises during biogenesis. Whether the observed misshapen variants are functionally impaired assembly "accidents" or represent intermediates that await processing to regular icosahedra remains to be determined. Mutants of α- and β-carboxysome containing bacteria that do not express the proposed vertex proteins are enriched in elongated carboxysomes (Price and Badger 1989, 1991; Price et al. 1993; Cai et al. 2009). Likewise, overexpression of a single shell protein of the Pdu BMC in *Salmonella enterica* cells leads to the production of normal as well as abnormally shaped particles (Havemann et al. 2002). Similar results were also reported in expression studies of the *pdu* operon of *Citrobacter freundii* in *E. coli* (Parsons et al. 2008). The BMCs of aberrant size and shape that are formed under these conditions suggest that a certain ratio of structural components is a crucial factor in the pathway that leads to the assembly of microcompartments of proper shape and size. Clearly, the expression of individual carboxysome proteins is closely regulated in vivo. In *H. neapolitanus,* a tight correlation exists between transcript levels for individual carboxysome proteins encoded by genes of the *cso* operon, and the abundance of each protein in the organelle (Cai et al. 2008).

4.8.1 Assembly Intermediates

Structures that likely represent α-carboxysome assembly intermediates were identified in a CET study of frozen, hydrated cells of *H. neapolitanus* (Iancu et al. 2010). The structures resemble partial shells at various stages of assembly; some, but not all of them, appear to be connected to one or more layers of RubisCO holoenzyme molecules on their concave sides. A structure that might be interpreted as a preassembled RubisCO core was not seen in any of the numerous cells examined in that study. Instead, the observed structures and the arrangement of the encapsulated RubisCO support a biogenesis pathway for α-carboxysome in which shell formation and the filling of nascent particles with RubisCO take place simultaneously. This model of carboxysome biogenesis is further supported by the polyhedral shells that are formed in a *H. neapolitanus* RubisCO knockout mutant and can be purified by sucrose gradient centrifugation (Menon et al. 2008). Although α-carboxysome shell

assembly and packaging of RubisCO are clearly independent processes (Menon et al. 2008), in vivo both must be coordinated and take place concomitantly during carboxysome formation. It is interesting that only one partially assembled carboxysome structure per cell was observed by Iancu et al. (2010), suggesting that a rate-determining nucleation event governs shell assembly and/or that the energetics of autotrophic metabolism limit the synthetic potential of the cell and the number of microcompartments that can be assembled at any given time.

In contrast to the single intermediates evident in *H. neapolitanus* cells, multiple small ring structures were seen in fixed and stained thin sections of the filamentous cyanobacterium *Anabaena variabilis* M3 (Price and Badger 1991). Their electron-translucent interior led to the suggestion that RubisCO and presumably also the carboxysomal carbonic anhydrase(s) enter a preassembled shell during carboxysome biogenesis in this cyanobacterium. For the unicellular cyanobacterium *Synechococcus elongatus* PCC 7942, an alternative model was proposed. Orus et al. (1995) found TEM evidence for supramolecular RubisCO assemblies that suggest shell formation occurs around an existing RubisCO core. This latter assembly model has gained support recently through a series of elegant genetic, biochemical, and cell biological studies that have established the pathway of β-carboxysome biogenesis in this cyanobacterium (Cameron et al. 2013).

4.8.2 The β-Carboxysome Assembly Pathway

Making use of an inducible shell protein operon in combination with fluorescently tagged individual shell proteins and RubisCO (Figure 4.4), Cameron et al. (2013) generated a series of single gene mutants that provided experimental evidence for the role of the major β-carboxysome proteins in organelle biogenesis. The progression of carboxysome assembly in vivo and the fate of newly formed organelles were followed by time lapse fluorescence microscopy. As in the α-carboxysome-forming chemoautotroph *H. neapolitanus* (Iancu et al. 2010), only one new carboxysome is formed per *Synechococcus elongatus* PCC 7942 cell, beginning with a preassembled RubisCO core (termed pro-carboxysome) that, in most cells, is located at one of the poles (Cameron et al. 2013; Chen et al. 2013). These studies further concluded that precursors of new carboxysomes bud off the pro-carboxysome (Cameron et al. 2013) and/or are generated adjacent to a recently formed organelle (Chen et al. 2013). With time, the new carboxysomes migrate closer to the center of the cell and seem to persist beyond a single cell division cycle (Jain et al. 2012).

The proposed assembly mechanism for β-carboxysomes in *Synechococcus elongatus* PCC 7942 (Cameron et al. 2013) is shown in Figure 4.5. Crucial for the formation of the RubisCO nucleus of the pro-carboxysome is the presence of CcmM. The RbcS-like domains of its C-terminal portion are thought to stabilize the RubisCO assembly. Whether RubisCO is arranged in a paracrystalline array, as is favored in the current model (Cameron et al. 2013; Chen et al. 2013), remains to be determined. In accordance with prior biochemical evidence (Long et al. 2007,

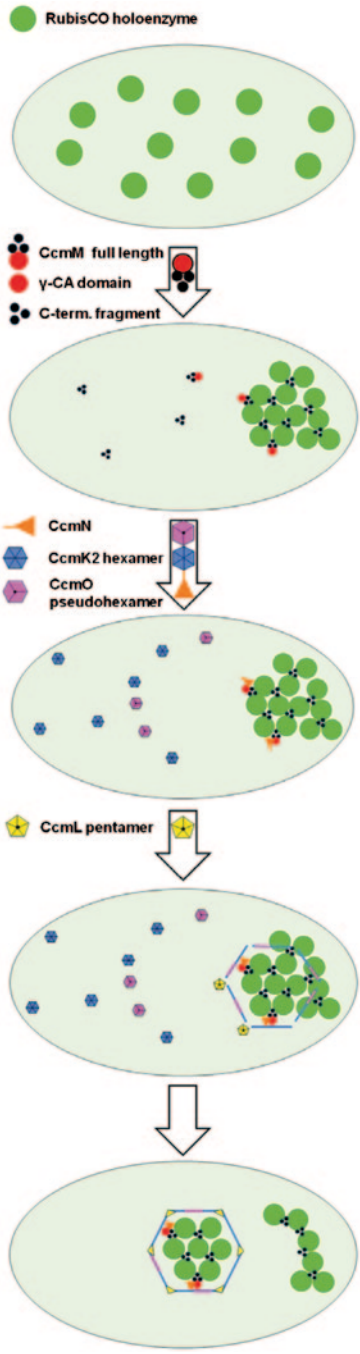

Fig. 4.5 The assembly pathway of β-carboxysomes. Carboxysome biogenesis begins with the assembly of a pro-carboxysome consisting of RubisCO and the CcmM full-length and C-terminal polypeptides. The CcmN protein recruits the shell proteins that self-assemble into the icosahedral carboxysome shell. Once completed, the newly generated carboxysome migrates towards the center of the cell. (Cameron et al. 2013)

2011; Cot et al. 2008; Kinney et al. 2012), the N-terminal domain of the full-length CcmM polypeptide binds to CcmN, which in turn recruits the Pfam00936 shell proteins CcmO and CcmK2 to the assembly, probably through interactions with its C-terminal peptide (Kinney et al. 2012). Incorporation of additional Pfam00936 proteins leads to formation of the hexamer arrays that constitute the shell facets. Addition of CcmL pentamers closes the shell at the vertices and is followed by the liberation of the completed carboxysome and its migration from its biogenesis site at the pole towards the center of the cell.

It is reasonable to assume that RubisCO must engage in specific contacts with shell component(s) during biogenesis of α- and β-carboxysomes, regardless of the assembly path. Although ultrastructural evidence obtained with purified α-carboxysomes could not unequivocally establish such interactions (Schmid et al. 2006; Iancu et al. 2007), the fact that only the Form IA RubisCO that is encoded by the *cso* operon of *Thiomicrospira crunogena*, but not its very similar non-carboxysomal paralog, can be encapsulated in *H. neapolitanus* carboxysomes (Menon et al. 2008) supports the existence of specific contacts with other carboxysome proteins. The large subunit of the enzyme has emerged as the determining factor for RubisCO encapsulation in α-carboxysomes. *H. neapolitanus* mutants expressing chimeric and foreign Form IA RubisCO species incorporate the enzyme into carboxysomes as long as the large subunit is derived from a carboxysomal RubisCO ortholog (Menon et al. 2008). Interestingly, α-carboxysomes can also accommodate Form IB RubisCO of β-carboxysomes (Menon et al. 2009), suggesting that any interactions of RubisCO with the shell transcend differences between the two carboxysome classes. It is noteworthy that extensive comparisons did not identify a sequence motif in the primary structure of carboxysomal RubisCOs that might target the enzymes into the carboxysome interior, such as the peptide that directs lumenal enzymes into the Pdu BMC (Fan et al. 2012). Regardless of the mechanism by which the carboxysomal RubisCO is sequestered into the organelle interior, there seems to be considerable flexibility regarding the nature of the cargo protein(s), since a GFP variant fused to the small subunit of RubisCO is readily incorporated into α-carboxysomes *H. neapolitanus* (Menon et al. 2010) and localizes to the punctuate fluorescent structures that are thought to represent individual β-carboxysomes in *Synechococcus elongatus* PCC 7942 when fused to the large subunit (RbcL; Savage et al. 2010; Cameron et al. 2013).

4.9 Carboxysome Segregation

The close to even distribution of carboxysomes within the two halves of dividing *H. neapolitanus* cells suggested the existence of an active distribution mechanism that ensures adequate CO_2 fixation potential in both daughter cells (Iancu et al. 2010). Although the exact molecular basis for such a mechanism is currently unknown, components of the bacterial cytoskeleton, which organize and/or move intracellular

structures (Jensen 1984; Gitai 2005), were considered likely candidates. Considering the close proximity of carboxysomes to DNA fibrils, which was noted in several bacteria (Mahoney and Edwards 1966; Gantt and Conti 1969; Shively et al. 1970, 1973; Purohit et al. 1976), it is not surprising that a protein implicated in DNA segregation was shown to play a role in partitioning carboxysomes among the daughter cells upon cell division. In *Synechococcus elongatus* PCC7942, in vivo tracking of fluorescently labeled carboxysomes revealed that carboxysomes are regularly interspersed with the multiple chromosome copies along the longitudinal cell axis of this bacterium (Jain et al. 2012). Mutants lacking the cytoskeletal protein ParA maintain the regular chromosome spacing (Jain et al. 2012), but their carboxysomes are not aligned like those in the wild type (Savage et al. 2010; Jain et al. 2012). These observations led the authors to suggest that ParA may utilize the ordered chromosomes to position carboxysomes in the cell or that, alternatively, chromosome spacing may restrict and therefore dictate the cellular locations of carboxysomes (Jain et al. 2012).

Following division, carboxysomes are not evenly apportioned to the two daughter cells in the Δ*par*A mutant, giving rise to cell subpopulations of normal fitness as well as those with reduced CO_2 fixation ability because they received an insufficient number of carboxysomes (Savage et al. 2010). The underlying molecular mechanism of ParA action is not known at present, and additional cytoskeletal components, such as MreB, also appear to participate in carboxysome organization and distribution (Savage et al. 2010). The frequent clustering and less regular intracellular spacing of carboxysomes seen in many chemo- and photoautotrophic bacteria raise the possibility that multiple organelle organization and segregation mechanisms may exist among the bacteria. It is noteworthy in this context that a *par*A homolog is present downstream from the *cso* operon of *H. neapolitanus* and of many other chemoautotrophs; whether its product plays a role in carboxysome ordering and movement remains to be elucidated.

4.10 Concluding Remarks

The wide range of fresh and increasingly sophisticated experimental approaches that have been applied to carboxysome research in recent years have produced considerable advances in the field. Our knowledge base of the relationship between structure and function of the organelle has greatly expanded; however, many of the questions that were summarized in a recent review (Kerfeld et al. 2010) still remain unanswered despite these great strides made towards gaining a complete understanding of carboxysome biology.

Similarities and differences between carboxysomes of the α- and β-type have become evident, thanks to novel insights into the roles and interactions of protein components that are unique to each type. It is clear that the two types of carboxysomes arose from different evolutionary events, and that they represent morphologically similar but compositionally different solutions to the problem of concentrating

CO_2 around the catalytically challenged RubisCO. Since the shell architecture of carboxysomes and other BMCs is very similar, comparative studies of BMC properties are needed that can elucidate unifying functions of BMCs and the principles of metabolic organization to which BMCs contribute.

For decades, the composition of α-carboxysomes, which can be purified to homogeneity, was assumed to have been elucidated. However, the recent discovery that the CsoS1D protein, which is not encoded in the canonical *cso* operon, is a low abundance shell component raises the possibility that other, as yet unknown proteins may be present and/or play a role in function, biogenesis, or regulation of both carboxysome types. Determination of structure and function of these, as well as other, less tractable carboxysome components is needed. An example of a still poorly understood component of α-carboxysomes is CsoS2, the largest and highly abundant shell protein. Technical difficulties related to its unusual characteristics have so far prevented elucidation of CsoS2 structure and role in the organelle.

For both carboxysome types, details of their shell properties remain to be resolved. To validate the proposed differential permeability of the shell to gases, experiments that directly address gas flux across the shell are required. Preferential CO_2 sequestration into the carboxysome interior and exclusion of O_2, the competitive inhibitor of the RubisCO-catalyzed carboxylation reaction, are elements of the prevailing working model and its variants. However, the molecular details of the proposed selective shell permeability and of metabolite transfer across the protein boundary remain a mystery.

Acknowledgments The authors are grateful to Drs. Fei Cai, Cheryl Kerfeld, Cristina Iancu, and Grant Jensen for the images they provided and their help with various figures in this review. We truly appreciate the many stimulating discussions we have had throughout the years of our respective collaborations. SH and GCC acknowledge the generous funding of their carboxysome research from the National Science Foundation (current awards: MCB-0851070 and MCB-1244534).

References

Alber BE, Ferry JG (1994) A carbonic anhydrase from the archaeon Methanosarcina thermophila. Proc Natl Acad Sci USA 91:6909–6913

Baker SH, Lorbach SC, Rodriguez-Buey M, Williams DS, Aldrich HC, Shively JM (1999) The correlation of the gene csoS2 of the carboxysome operon with two polypeptides of the carboxysome in Thiobacillus neapolitanus. Arch Microbiol 172:233–239

Baker SH, Williams DS, Aldrich HC, Gambrell AC, Shively JM (2000) Identification and localization of the carboxysome peptide CsoS3 and its corresponding gene in Thiobacillus neapolitanus. Arch Microbiol 173:278–283

Berry S, Fischer JH, Kruip J, Hauser M, Wildner GF (2005) Monitoring cytosolic pH of carboxysome-deficient cells of Synechocystis sp. PCC 6803 using fluorescence analysis. Plant Biol (Stuttg) 7:342–347

Beudeker RF, Cannon GC, Kuenen JG, Shively JM (1980) Relations between d-ribulose-1,5-bisphosphate carboxylase, carboxysomes, and CO_2 fixing capacity in the obligate chemolithotroph Thiobacillus neapolitanus grown under different limitations in the chemostat. Arch Microbiol 124:185–189

Bobik TA (2006) Polyhedral organelles compartmenting bacterial metabolic processes. Appl Microbiol Biotechnol 70:517–525

Bock E, Duval D, Peters KR (1974) Charakterisierung eines phagenähnlichen Partikels aus Zellen von Nitrobacter. I. Wirstpartikelbeziehung und Isolierung. Arch Microbiol 97:115–127

Cai F, Heinhorst S, Shively J, Cannon G (2008) Transcript analysis of the Halothiobacillus neapolitanus cso operon. Arch Microbiol 189:141–150

Cai F, Menon BB, Cannon GC, Curry KJ, Shively JM, Heinhorst S (2009) The pentameric vertex proteins are necessary for the icosahedral Carboxysome shell to function as a CO_2 leakage barrier. PLoS ONE 4:e7521

Cai F, Sutter M, Cameron JC, Stanley DN, Kinney JN, Kerfeld CA (2013) The structure of CcmP, a tandem bacterial microcompartment domain protein from the beta-carboxysome, forms a subcompartment within a microcompartment. J Biol Chem 288:16055–16063

Cameron JC, Wilson SC, Bernstein SL, Kerfeld CA (2013) Biogenesis of a bacterial organelle: the carboxysome assembly pathway. Cell 155:1131–1140

Cannon GC, Shively JM (1983) Characterization of a homogenous preparation of carboxysomes from Thiobacillus neapolitanus. Arch Microbiol 134:52–59

Cannon GC, Heinhorst S, Bradburne CE, Shively JM (2002) Carboxysome genomics: a status report. Funct Plant Biol 29:175–182

Cannon GC, Baker SH, Soyer F, Johnson DR, Bradburne CE, Mehlman JL, Davies PS, Jiang QL, Heinhorst S, Shively JM (2003) Organization of carboxysome genes in the thiobacilli. Curr Microbiol 46:115–119

Cannon GC, Heinhorst S, Kerfeld CA (2010) carboxysomal carbonic anhydrases: structure and role in microbial CO_2 fixation. Biochim Biophys Acta 1804:382–392

Chen AH, Robinson-Mosher A, Savage DF, Silver PA, Polka JK (2013) The bacterial carbon-fixing organelle is formed by shell envelopment of preassembled cargo. PLoS ONE 8:e76127

Cheng S, Liu Y, Crowley CS, Yeates TO, Bobik TA (2008) Bacterial microcompartments: their properties and paradoxes. Bioessays 30:1084–1095

Cot SS-W, So AK-C, Espie GS (2008) A multiprotein bicarbonate dehydration complex essential to carboxysome function in cyanobacteria. J Bacteriol 190:936–945

Dou Z, Heinhorst S, Williams EB, Murin CD, Shively JM, Cannon GC (2008) CO_2 fixation kinetics of *Halothiobacillus neapolitanus* mutant carboxysomes lacking carbonic anhydrase suggest the shell acts as a diffusional barrier for CO_2. J Biol Chem 283:10377–10384

Fan C, Cheng S, Liu Y, Escobar CM, Crowley CS, Jefferson RE, Yeates TO, Bobik TA. (2012) Short N-terminal sequences package proteins into bacterial microcompartments. Proc Natl Acad Sci USA 107:7509–7514

Gantt E, Conti SF (1969) Ultrastructure of blue-green algae. J Bacteriol 97:1486–1493

Gitai Z (2005) The new bacterial cell biology: moving parts and subcellular architecture. Cell 120:577–586

de Groot BL, Grubmuller H (2005) The dynamics and energetics of water permeation and proton exclusion in aquaporins. Curr Opin Struct Biol 15:176–183

Havemann GD, Sampson EM, Bobik TA (2002) PduA is a shell protein of polyhedral organelles involved in coenzyme B(12)-dependent degradation of 1,2-propanediol in *Salmonella enterica* serovar typhimurium LT2. J Bacteriol 184:1253–1261

Heinhorst S, Cannon GC, Shively JM (2006) Carboxysomes and carboxysome-like inclusions. In: Shively JM (ed) Complex intracellular structures in prokaryotes, vol 2. Springer, Berlin, pp 141–164

Heinhorst S, Williams EB, Cai F, Murin CD, Shively JM, Cannon GC (2006) Characterization of the carboxysomal carbonic anhydrase CsoSCA from *Halothiobacillus neapolitanus*. J Bacteriol 188:8087–8094

Holthuijzen YA, Breemen JFL, Konings WN, Bruggen EFJ (1986) Electron microscopic studies of carboxysomes of *Thiobacillus neapolitanus*. Arch Microbiol 144:258–262

Iancu CV, Ding HJ, Morris DM, Dias DP, Gonzales AD, Martino A, Jensen GJ (2007) The structure of isolated synechococcus strain WH8102 Carboxysomes as revealed by electron cryotomography. J Mol Biol 372:764–773

Iancu CV, Morris DM, Dou Z, Heinhorst S, Cannon GC, Jensen GJ (2010) Organization, structure, and assembly of [alpha]-carboxysomes determined by electron cryotomography of intact cells. J Mol Biol 396:105–117

Jain IH, Vijayan V, O'Shea EK (2012) Spatial ordering of chromosomes enhances the fidelity of chromosome partitioning in cyanobacteria. Proc Natl Acad Sci USA 109:13638–13643

Jensen TE (1984) Cyanobacterial cell inclusions of irregular occurrence: systematic and evolutionary implications. Cytobios 39:35–62

Kaneko Y, Danev R, Nagayama K, Nakamoto H (2006) Intact carboxysomes in a cyanobacterial cell visualized by hilbert differential contrast transmission electron microscopy. J Bacteriol 188:805–808

Kaplan A, Reinhold L (1999) CO_2 concentrating mechanisms in photosynthetic microorganisms. Annu Rev Plant Physiol Plant Mol Biol 50:539–570

Kerfeld CA, Sawaya MR, Tanaka S, Nguyen CV, Phillips M, Beeby M, Yeates TO (2005) Protein structures forming the shell of primitive bacterial organelles. Science 309:936–938

Kerfeld CA, Heinhorst S, Cannon GC (2010) Bacterial microcompartments. Annu Rev Microbiol 64:391–408

Kinney J, Axen S, Kerfeld CA (2011) Comparative analysis of carboxysome shell proteins. Photosynth Res 109:21–32

Kinney JN, Salmeen A, Cai F, Kerfeld CA (2012) Elucidating essential role of conserved carboxysomal protein CcmN reveals common feature of bacterial microcompartment assembly. J Biol Chem 287:17729–17736

Klein MG, Zwart P, Bagby SC, Cai F, Chisholm SW, Heinhorst S, Cannon GC, Kerfeld CA (2009) Identification and structural analysis of a novel carboxysome shell protein with implications for metabolite transport. J Mol Biol 392:319–333

Liberton M, Austin JR, Berg RH, Pakrasi HB (2011) Unique thylakoid membrane architecture of a unicellular N_2-fixing cyanobacterium revealed by electron tomography Plant Physiol 155:1656–1666

Long BM, Price GD, Badger MR (2005) Proteomic assessment of an established technique for carboxysome enrichment from Synechococcus PCC7942. Can J Bot 83:746–757

Long BM, Badger MR, Whitney SM, Price GD (2007) Analysis of carboxysomes from Synechococcus PCC7942 reveals multiple RubisCO complexes with carboxysomal proteins CcmM and CcaA. J Biol Chem 282:29323–29335

Long BM, Tucker L, Badger MR, Price GD (2010) Functional cyanobacterial β-carboxysomes have an absolute requirement for both long and short forms of the CcmM protein. Plant Physiol 153:285–293

Long BM, Rae BD, Badger MR, Price GD (2011) Over-expression of the β-carboxysomal CcmM protein in Synechococcus PCC7942 reveals a tight co-regulation of carboxysomal carbonic anhydrase (CcaA) and M58 content. Photosynth Res 109:33–45

Ludwig M, Sültemeyer D, Price GD (2000) Isolation of ccmKLMN genes from the marine cyanobacterium Synechococcus sp. PCC7002 and evidence that CcmM is essential for carboxysome assembly. J Phycol 36:1109–1118

Mahoney RP, Edwards MR (1966) Fine structure of *Thiobacillus thiooxidans*. J Bacteriol 92: 487–495

McKay RML, Gibbs SP, Espie GS (1993) Effect of dissolved inorganic carbon on the expression of carboxysomes, localization of RubisCO and the mode of carbon transport in cells of the cyanobacterium Synechococcus UTEX 625. Arch Microbiol 159:21–29

Menon BB, Dou Z, Heinhorst S, Shively JM, Cannon GC (2008) *Halothiobacillus neapolitanus* carboxysomes sequester heterologous and chimeric RubisCO species. PLoS ONE 3:e3570

Menon BB, Dou Z, Milam J, Shively JM, Heinhorst S, Cannon GC (2009) Phenotypic analysis of a Halothiobacillus neapolitanus mutant harboring beta-cyanobacterial form IB RubisCO. In: Amercian society for microbiology 109th general meeting Philadelphia, PA. K–066

Menon BB, Heinhorst S, Shively JM, Cannon GC (2010) The carboxysome shell is permeable to protons. J Bacteriol 192:5881–5886

Nierzwicki-Bauer S, Balkwill D, Stevens S Jr (1983) Three-dimensional ultrastructure of a unicellular cyanobacterium. J Cell Biol 97:713–722

Orus MI, Rodriguez ML, Martinez F, Marco E (1995) Biogenesis and ultrastructure of carboxysomes from wild type and mutants of Synechococcus sp. strain PCC 7942. Plant Physiol 107:1159–1166

Orus MI, Rodriguez-Buey ML, Marco E, Fernandez-Valiente E (2001) Changes in carboxysome structure and grouping and in photosynthetic affinity for inorganic carbon in Anabaena strain PCC 7119 (Cyanophyta) in response to modification of CO_2 and Na^+ supply. Plant Cell Physiol 42:46–53

Parsons JB, Dinesh SD, Deery E et al (2008) Biochemical and structural insights into bacterial organelle form and biogenesis. J Biol Chem 283:14366–14375

Peña KL, Castel SE, de Araujo C, Espie GS, Kimber MS (2010) Structural basis of the oxidative activation of the carboxysomal gamma-carbonic anhydrase, CcmM. Proc Natl Acad Sci USA 107:2455–2460

Penrod JT, Roth JR (2006) Conserving a volatile metabolite: a role for carboxysome-like organelles in *Salmonella enterica*. J Bacteriol 188:2865–2874

Peters K-R (1974) Characterisierung eines phagenaehnlichen Partikels aus Zellen von Nitrobacter. Arch Microbiol 97:129–140

Price GD, Badger MR (1989) Isolation and characterization of high CO_2-requiring-mutants of the cyanobacterium Synechococcus PCC 7942: two phenotypes that accumulate inorganic carbon but are apparently unable to generate CO_2 within the carboxysome. Plant Physiol 91:514–525

Price GD, Badger MR (1991) Evidence for the role of carboxysomes in the cyanobacterial CO_2-concentrating mechanism. Can J Bot 69:963–973

Price GD, Coleman JR, Badger MR (1992) Association of carbonic anhydrase activity with carboxysomes isolated from the cyanobacterium Synechococcus PCC7942. Plant Physiol 100:784–793

Price GD, Howitt S, Harrison K, Badger MR (1993) Analysis of a genomic DNA region from the cyanobacterium Synechococcus sp. strain PCC7942 involved in carboxysome assembly and function. J Bacteriol 175:2871–2879

Price GD, Sültemeyer D, Klughammer B, Ludwig M, Badger MR (1998) The functioning of the CO_2 concentrating mechanism in several cyanobacterial strains: a review of general physiological characteristics, genes, proteins and recent advances. Can J Bot 76:973–1002

Pronk JT, Meulenberg R, van den Berg DJ, Batenburg-van der Vegte W, Bos P, Kuenen JG (1990) Mixotrophic and autotrophic growth of *Thiobacillus acidophilus* on glucose and thiosulfate. Appl Environ Microbiol 56:3395–3401

Purohit K, McFadden BA, Shaykh MM (1976) D-Ribulose-1,5-bisphosphate carboxylase and polyhedral inclusion bodies in *Thiobacillus intermedius*. J Bacteriol 127:516–522

Rae BD, Long BM, Badger MR, Price GD (2012) Structural determinants of the outer shell of β-carboxysomes in *Synechococcus elongatus* PCC 7942: roles for CcmK2, K3-K4, CcmO, and CcmL. PLoS ONE 7:e43871

Rae BD, Long BM, Badger MR, Price GD (2013) Functions, compositions, and evolution of the two types of carboxysomes: polyhedral microcompartments that facilitate CO_2 fixation in cyanobacteria and some proteobacteria. Microbiol Mol Biol Rev 77: 357–379

Reinhold L, Zviman M, Kaplan A (1989) A quantitative model for carbon fluxes and photosynthesis in cyanobacteria. Plant Physiol Biochem 27:945–954

Roberts EW, Cai F, Kerfeld CA, Cannon GC, Heinhorst S (2012) Isolation and characterization of the prochlorococcus carboxysome reveal the presence of the novel shell protein CsoS1D. J Bacteriol 194:787–795

Samborska B, Kimber MS (2012) A dodecameric CcmK2 structure suggests beta-carboxysomal shell facets have a double-layered organization. Structure 20:1353–1362

Savage DF, Afonso B, Chen AH, Silver PA (2010) Spatially ordered dynamics of the bacterial carbon fixation machinery. Science 327:1258–1261

Sawaya MR, Cannon GC, Heinhorst S, Tanaka S, Williams EB, Yeates TO, Kerfeld CA (2006) The structure of β-carbonic anhydrase from the carboxysomal shell reveals a distinct subclass with one active site for the price of two. J Biol Chem 281:7546–7555

Schmid MF, Paredes AM, Khant HA, Soyer F, Aldrich HC, Chiu W, Shively JM (2006) Structure of *Halothiobacillus neapolitanus* carboxysomes by cryo-electron tomography. J Mol Biol 364:526–535

Shepherd CM, Borelli IA, Lander G, Natarajan P, Siddavanahalli V, Bajaj C, Johnson JE, Brooks CL 3rd, Reddy VS (2006) VIPERdb: a relational database for structural virology. Nucl Acids Res 34:D386–389

Shively JM, English RS (1991) The carboxysome, a prokaryotic organelle: a mini review. Can J Bot 69:957–962

Shively JM, Decker GL, Greenawalt JW (1970) Comparative ultrastructure of the thiobacilli. J Bacteriol 101: 618–627

Shively JM, Ball F, Brown DH, Saunders RE (1973a) Functional organelles in prokaryotes: polyhedral inclusions (carboxysomes) of *Thiobacillus neapolitanus*. Science 182:584–586

Shively JM, Ball FL, Kline BW (1973b) Electron microscopy of the carboxysomes (polyhedral bodies) of *Thiobacillus neapolitanus*. J Bacteriol 116:1405–1411

So AK-C, Espie GS (1998) Cloning, characterization and expression of carbonic anhydrase from the cyanobacterium Synechocystis PCC6803. Plant Mol Biol 37:205–215

So AK-C, John-McKay M, Espie GS (2002) Characterization of a mutant lacking carboxysomal carbonic anhydrase from the cyanobacterium Synechocystis PCC6803. Planta 214:456–467

So AK-C, Espie GS, Williams EB, Shively JM, Heinhorst S, Cannon GC (2004) A novel evolutionary lineage of carbonic anhydrase (epsilon class) is a component of the carboxysome shell. J Bacteriol 186:623–630

Tanaka S, Kerfeld CA, Sawaya MR, Cai F, Heinhorst S, Cannon GC, Yeates TO (2008) Atomic-level models of the bacterial carboxysome shell. Science 319:1083–1086

Tanaka S, Sawaya MR, Phillips M, Yeates TO (2009) Insights from multiple structures of the shell proteins from the beta-carboxysome. Protein Sci 18:108–120

Tang M, Jensen TE, Corpe WA (1995) The occurrence of polyphosphate bodies in polyhedral bodies (carboxysomes) in *Synechococcus leopoliensis* (Cyanophyceae). Microbios 81:59–66

Ting CS, Hsieh C, Sundararaman S, Mannella C, Marko M (2007) Cryo-electron tomography reveals the comparative three-dimensional architecture of Prochlorococcus, a globally important marine cyanobacterium. J Bacteriol 189:4485–4493

Tocheva EI, Li Z, Jensen GJ (2010) Electron cryotomography. Cold Spring Harb Perspect Biol 2:a003442

Tsai Y, Sawaya MR, Cannon GC, Cai F, Williams EB, Heinhorst S, Kerfeld CA, Yeates TO (2007) Structural analysis of CsoS1A and the protein shell of the *Halothiobacillus neapolitanus* carboxysome. PLoS Biol 5:e144

Tsai Y, Sawaya MR, Yeates TO (2009) Analysis of lattice-translocation disorder in the layered hexagonal structure of carboxysome shell protein CsoS1C. Acta Crystallogr D Biol Crystallogr 65:980–988

van der Meene AML, Hohmann-Marriott MF, Vermaas WFJ, Roberson RW (2006) The three-dimensional structure of the cyanobacterium Synechocystis sp. PCC 6803. Arch Microbiol 184:259–270

Westphal K, Bock E (1974) Charakterisierung eines phagenähnlichen Partikels aus Zellen von Nitrobacter III. Nachweis von DNS. Arch Microbiol 101:121–130

Yeates TO, Kerfeld CA, Heinhorst S, Cannon GC, Shively JM (2008) Protein-based organelles in bacteria: carboxysomes and related microcompartments. Nat Rev Microbiol 6:681–691

Yeates TO, Thompson MC, Bobik TA (2011) The protein shells of bacterial microcompartment organelles. Curr Opin Struct Biol 21:223–231

Yeates TO, Jorda J, Bobik TA (2013) The shells of BMC-type microcompartment organelles in bacteria. J Mol Microbiol Biotechnol 23:290–299

Zhang S, Laborde SM, Frankel LK, Bricker TM (2004) Four novel genes required for optimal photoautotrophic growth of the cyanobacterium Synechocystis sp. strain PCC 6803 identified by in vitro transposon mutagenesis. J Bacteriol 186:875–879